Structural Model of a Synthetic Ca^{2+} Channel with Bound Ca^{2+} Ions and Dihydropyridine Ligand

Boris S. Zhorov and Vettai S. Ananthanarayanan
Department of Biochemistry, McMaster University, Hamilton, Ontario, Canada L8N 3Z5

ABSTRACT Grove et al. have demonstrated L-type Ca^{2+} channel activity of a synthetic channel peptide (SCP) composed of four helices (sequence: DPWNVFDFLI^{10}VIGSIIDVIL^{20}SE) tethered by their C-termini to a nanopeptide template. We sought to obtain the optimal conformations of SCP and locate the binding sites for Ca^{2+} and for the dihydropyridine ligand nifedipine. Eight Ca^{2+} ions were added to neutralize the 16 acidic residues in the helices. Eight patterns of the salt bridges between Ca^{2+} ions and pairs of the acidic residues were calculated by the Monte Carlo-with-energy-minimization (MCM) protocol. In the energetically optimal conformation, two Ca^{2+} ions were bound to Asp-1 residues at the intracellular side of SCP, and six Ca^{2+} ions were arrayed in two files at the diametrically opposite sides of the pore, implying a Ca^{2+} relay mechanism. Nine modes of nifedipine binding to SCP were simulated by the MCM calculations. In the energetically optimal mode, the ligand fits snugly in the pore. The complex is stabilized by Ca^{2+} bound between two Asp-17 residues and hydrophilic groups of the ligand. The latter substitute water molecules adjacent to Ca^{2+} in the ligand-free pore and thus do not obstruct Ca^{2+} relay. The ligand-binding site is proximal to a hydrophobic bracelet of Ile-10 residues whose rotation is sterically hindered. In some conformations, the bracelet is narrow enough to block the permeation of the hydrated Ca^{2+} ions. The bracelet may thus act as a "gate" in SCP. Nifedipine and (*R*)-Bay K 8644, which act as blockers of the SCP, extend a side-chain hydrophobic moiety toward the Ile-10 residues. This would stabilize the pore-closing conformation of the gate. In contrast, the channel activator (*S*)-Bay K 8644 exposes a hydrophilic moiety toward the Ile-10 residues, thus destabilizing the pore-closing conformation of the gate.

INTRODUCTION

Ca^{2+} channels modulate the movement of Ca^{2+} in excitable cells. In spite of intensive study, the molecular mechanisms of ion selectivity and pharmacological sensitivity of Ca^{2+} channels are unclear. This is mainly due to the lack of structural information on these channels. Such information is necessary to understand the general principles of the Ca^{2+} channels' organization, a goal important for basic knowledge and medicinal applications. By their physiological characteristics, Ca^{2+} channels are divided into T-, L-, N-, and P-types. The L-type Ca^{2+} channels that mediate the inward movement of Ca^{2+} in cardiac and smooth muscle cells are the best characterized among the four types of the Ca^{2+} channels. The L-type channel is composed of five subunits, α_1, α_2, β, γ, and δ. The pore is formed by the α_1-subunit, the other subunits having a regulatory role. The α_1-subunit incorporates four domains, I–IV. The folding pattern of each domain was predicted to comprise six membrane-spanning segments (S1–S6) and two short segments SS1 and SS2 in the S5-S6 linker, which span the membrane only partially. The α_1-subunit incorporates receptors for the well-known Ca^{2+} channel ligands: phenylalkylamines, benzothiazepines, and 4-aryl-1,4-dihydropyridines. Some of these ligands are used as drugs for the treatment of cardiovascular diseases. In spite of a large body of information on these drugs, the molecular mechanism of their action at the Ca^{2+} channels remains unknown. In particular, the intriguing fact that the (*R*)-enantiomer of the dihydropyridine, Bay K 8644, decreases the open state probability of the L-type Ca^{2+} channel whereas the (*S*)-enantiomer increases it remains to be explained.

Earlier we hypothesized that Ca^{2+} channels may form ternary complexes with Ca^{2+} and the ligands (Zhorov and Govyrin, 1984, 1985; Ananthanarayanan, 1991a,b). Recent data show that the Ca^{2+} channel ligands verapamil, diltiazem, nicardipine, and nifedipine bind Ca^{2+} in a nonpolar lipid-mimicking environment (Ananthanarayanan et al., 1992, 1993; Tetreault and Ananthanarayanan, 1993; Belciug and Ananthanarayanan, 1994). The fact that phenylalkylamines and benzothiazepines incorporate amino groups that are predominantly protonated at physiological pH complies with the possibility of their binding inside the cation-selective pore of the L-type channel. Contrarily, dihydropyridines (DHPs) that are predominantly in a neutral form at physiological pH were speculated to bind at the channel-lipid interface (Kokubun et al., 1986) to the basic amino acids of the voltage sensor (Langs et al., 1990) at the cytoplasmic domain adjacent to IVS6 (Regulla et al., 1991). However, recent experiments suggest that DHP receptor is located either close to the extracellular entry of the pore (Kass et al., 1991; Strubing et al., 1993; Tang et al., 1993)

Received for publication 19 May 1995 and in final form 22 September 1995.

Address reprint requests to Dr. Vettai S. Ananthanarayanan, Department of Biochemistry, McMaster University, Hamilton, Ontario L8N 3Z5 Canada. Tel.: 905-525-9140 X22783; Fax: 905-522-9033; E-mail: ananth@fhs.mcmaster.ca.

Dr. Zhorov is on leave from the Sechenov Institute of Evolutionary Physiology and Biochemistry of the Russian Academy of Sciences. Present address: Sechenov Institute of Evolutionary Physiology and Biochemistry, St. Petersburg, 194223, Russia. E-mail: zhorov@ief.spb.su.

© 1996 by the Biophysical Society

0006-3495/96/01/22/16 $2.00

or inside the pore (Kalasz et al., 1993). DHPs bind to their receptor in a Ca^{2+}-dependent way (Glossman and Ferry, 1983; Gould et al., 1984; Flockerzi et al., 1986; Knaus et al., 1992). However, the structural interpretation of these experiments for a complex protein with unknown three-dimensional structure is problematic. Studies using simpler synthetic analogs of the channel are therefore desirable.

Grove et al. (1991) designed a synthetic calcium channel peptide (SCP) composed of four α-helical segments, each having the sequence found in the IVS3 transmembrane segment of the cardiac L-type Ca^{2+} channel: DPWNVFDFLI[10]VIGSIIDVIL[20]SE (Mikami et al., 1989). The four helices were tethered by their carboxy termini to a nanopeptide template: KKKPGKEKG. The authors demonstrated that the effects of the (*S*)- and (*R*)-enantiomers of Bay K 8644 as well as some other drugs and metal ions at SCP are similar to those at the L-type channel (Grove et al., 1991, 1993). In the absence of the basic amino acids in the transmembrane segments, ionized Asp and Glu residues are the most probable candidates in SCP to interact with DHPs and Ca^{2+} in the ternary complex. Other interactions may include hydrogen bonding of DHPs to the channel directly or via water molecules. Hydrophilic residues of the SCP should face the interior of the pore to constitute a path for the permeating Ca^{2+}. On the other hand, the exposure of the hydrophilic residues of the four-helix bundle to the lipid bilayer will be energetically unfavorable. The DHPs would therefore be bound inside the hydrophilic pore of the four-helix bundle. The puzzling question is why DHPs bound inside the narrow pore do not block it but modulate (increase or decrease) the probability of the channel's closed state. Molecular modeling is an appropriate approach to answering this question.

Because SCP is much smaller than the α_1-subunit of the L-type channel and has a relatively well-defined four-helix bundle topology, computer simulation of the former is feasible. In this work, molecular modeling was applied to find the optimal conformations of the SCP with Ca^{2+} ions, to locate the binding sites for the DHP ligand nifedipine inside the pore, and to estimate the energies of different modes of nifedipine binding. The results obtained predict the detailed structure of the four-helix bundle and suggest a mechanism for the selectivity of the channel to Ca^{2+} ions versus monovalent cations. They also demonstrate the ternary association of SCP with nifedipine and Ca^{2+} and present an explanation for the opposite effects of the (*R*)- and (*S*)-enantiomers of Bay K 8644 on the channel. Because SCP lacks the short segments SS1-SS2, the critical pore-forming elements of the authentic voltage-gated ion channels (Guy and Conti, 1990), the model of SCP is not expected to predict the detailed structure of the L-type Ca^{2+} channel pore. However, the proposed elementary mechanisms of ion permeation, ion selectivity, and pharmacological sensitivity of SCP may also be relevant to L-type Ca^{2+} channels. Preliminary results of this study have been published as an abstract (Zhorov and Ananthanarayanan, 1995).

MATERIALS AND METHODS

An ECEPP/2 force field (Momany et al., 1975; Nemethy et al., 1983) was used for calculations of the SCP and its complexes with Ca^{2+} and nifedipine. Electrostatic interactions were calculated with a distance-dependent dielectric ($\epsilon = r$). In the absence of parameters for Ca^{2+} in the ECEPP/2 force field, Ca^{2+} was modeled as an oxygen atom with a double proton charge (Zhorov, 1993; Zhorov and Ananthanarayanan, 1994). The interactions between Ca^{2+} ions, between Ca^{2+} ions and carboxylate groups, and between carboxylate groups were calculated at all of the distances. Other interactions were calculated with a cut-off distance of 7 Å. Energy calculations were carried out on the Indigo-2 Extreme workstation (Silicon Graphics) using the ZMM package (Zhorov, 1981, 1993). Energy was minimized in the space of generalized coordinates. The latter were categorized in two groups: the essential generalized coordinates (torsional angles specifying rotations of nonsymmetric groups, Cartesian coordinates specifying translations of Ca^{2+} ions and of the ligand, Euler angles specifying rotations of the ligand) and nonessential generalized coordinates (the torsions of the following symmetric groups: CH_3, COO, NH_2, NO_2, and C_6H_5). Bond lengths, bond angles, and aromatic rings were kept rigid. In the transmembrane segments, all backbone torsions, except those of Asp-1, were fixed in a preliminarily calculated α-helical conformation (see Results). It should be noted, however, that the torsions of the template nanopeptide, including side-chain torsions of Lys residues linking the nanopeptide to the transmembrane helices, were varied in the search for the optimal conformations, thus allowing variance of the spatial disposition of the helices relative to each other and relative to the nanopeptide template. Proline rings of the transmembrane segments were fixed in *trans-down* conformation (Momany et al., 1975). Structures were visualized using the Insight II (Biosym Inc.) package.

In the SCP molecule, the transmembrane segments connected to the Lys-1, Lys-3, Lys-6, and Lys-8 residues of the nanopeptide template KKKPGKEKG were designated H1, H2, H3, and H4, respectively. Four levels (A, B, C, and D) normal to the main axis of the four-helix bundle have been identified to contain, respectively, Glu-22, Asp-17, Asp-7, and Asp-1 (Fig. 1).

The Monte Carlo-with-energy-minimization (MCM) protocol (Li and Scheraga, 1988) was used for searching the optimal conformations. A

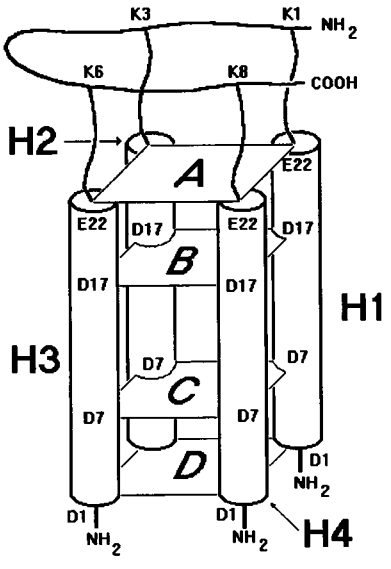

FIGURE 1 A sketch of the four-helical bundle of the SCP. The helices H1, H2, H3, H4 are tethered to Lys residues in the template nanopeptide. The template and the N-termini of the transmembrane segments are shown in thick lines. The planes A, B, C, and D indicate the levels of the acidic residues Glu-22, Asp-17, Asp-7, and Asp-1, respectively. The amino acid residues are labeled with the one-letter code for their names.

recent description of the method may be found in the study of Abagyan and Argos (1992). Trajectories were calculated at T = 600 K. An initial structure of a trajectory was usually constructed with the help of the graphical interface. Then the structure was imported in the ZMM program and energy was minimized until either the norm of the energy gradient become less than 1 kcal·mol^{-1}·rad^{-1} or the number of iterations exceeded 1000. A subsequent starting point in the trajectory was obtained by changing a randomly selected essential generalized coordinate G of the preceding point by a random increment D, where $D \in (-180°, 180°)$ if G was a torsional angle of the side-chain group or an Euler angle of the ligand, $D \in (-60°, 60°)$ if G was a torsional angle in the template backbone or in a chain tethering the transmembrane segments to the template, and $D \in (-4$ Å, 4 Å) if G was a Cartesian coordinate of Ca^{2+} or the ligand. From a given starting point, energy was minimized and the resulting minimum-energy conformation (MEC) was accepted in the trajectory if its energy E was less than that of the preceding point of the trajectory E_p, or, if a random number $n \in (0, 1)$ was less than $\exp(-(E - E_p)/RT)$.

In some cases, distances r between specified atoms were restrained within the boundaries $d_l < r < d_h$ by using the quasiparabolic function $E_r = s(r) * f(r)$, where $s(r)$ is a switching operator (Brooks et al., 1985):

$$s(r) = \begin{cases} 1 & \text{if } r \le d_l - x \\ [(d_l + x - r)^2(d_l + x - 3(d_l - x) + 2r)]/(2x)^3 & \text{if } d_l - x < r \le d_l + x \\ 0 & \text{if } d_l + x < r \le d_h - x \\ [(d_h - x - r)^2(x - d_h + 3(d_h + x) - 2r)]/(2x)^3 & \text{if } d_h - x < r \le d_h + x \\ 1 & \text{if } d_h + x < r, \end{cases}$$

and the penalty function

$$f(r) = C(r - d_h/2 - d_l/2)^2,$$

where x is the switching distance (0.2 Å) and C is the force constant (100 kcal mol^{-1} Å^{-2}). The restraints were used to impose salt bridges between Ca^{2+} ions and oxygen atoms (d_l = 2 Å, d_h = 3 Å) and to retain the four-helix bundle topology of the SCP by limiting the distances between the C^β atoms of Trp-3 residues in the diagonally oppositely spaced helices (d_l = 9 Å, d_h = 11 Å). In the simulations of the ligand binding to SCP, the optimal MECs found in the restrained MCM trajectories were used as the starting points for the subsequent nonrestrained MCM trajectories. Low-energy MECs found in each trajectory were accumulated in stacks (Zhorov and Ananthanarayanan, 1993). The stacks were used later for the search of the MECs meeting specified criteria, e.g., the distances between Ile-10 residues in different helices.

The convergence of a typical restrained MCM trajectory is shown in Fig. 2 in terms of the energy of the lowest MEC found during simulation as a function of the number of energy minimizations. The first MEC had a very high energy, indicating that bad contacts unavoidable in the starting conformation were not eliminated by a single energy minimization (the conformation was trapped in a high-energy region of the hyperspace). The next few hundred energy minimizations steadily decreased the energy, eliminating step by step the bad contacts. Further minimizations decreased the energy slowly and increased the number of the collected low-energy MECs. MCM trajectories were usually terminated when several hundred additional energy minimizations did not lower the energy of the current lowest MEC. Different trajectories had a similar tendency of convergence, the energy of the lowest MEC in the trajectory rarely decreasing after 1000 minimizations at the flat part of the trajectory. The acceptance ratio in the MCM simulations was 10–20%. Test calculations demonstrated that energy may further decrease, but not significantly. If a trajectory converged slowly and the energy remained high, this indicated that the specified restraints were inconsistent with the structure of the SCP. Such trajectories were terminated after a few hundred energy minimizations. Thus, an MCM trajectory yields an "almost" lowest MEC in the vicinity of the starting point but does not move the structure of the macromolecule in a region essentially different from the starting point (unlike MCM simulations of oligopeptides, which do). Different regions in the hyperspace of the SCP seem to be separated by large barriers, overcoming which requires the simultaneous readjustment of many contacts between helices and, hence, the variation of many generalized coordinates. A starting conformation in any step of the MCM trajectory may differ dramatically from the MEC

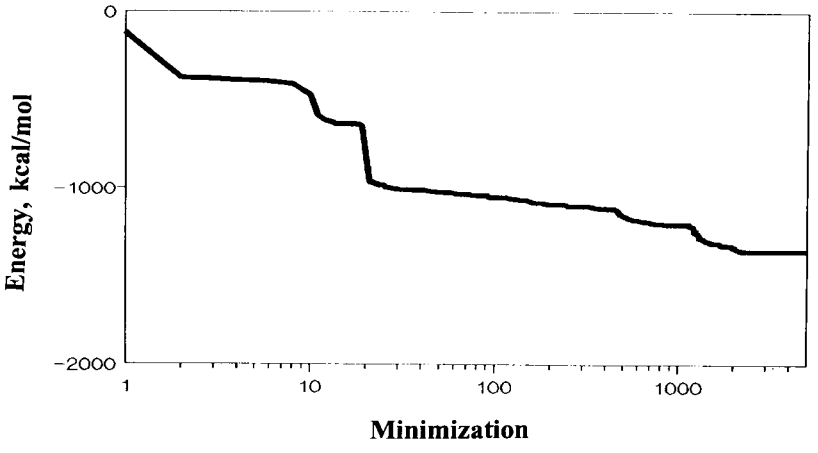

FIGURE 2 Convergence of a typical MCM trajectory of SCP. The energy of the current lowest MEC detected in the trajectory is shown as a function of number of energy minimizations.

accepted in the proceeding step (e.g., a change of a torsion in the template nanopeptide may essentially move a helix). The subsequent single energy minimization may eliminate bad contacts, but it cannot establish an optimal set of new contacts between the side chains of the helices, resulting in MECs with relatively high energy. In the protocol used, such high-energy MECs were not accepted into the trajectory. This is the reason for the relatively low acceptance ratio. The main advantage of the protocol used is that even very bad starting conformations converged reliably to the low-energy MECs.

RESULTS AND DISCUSSION

Structure of SCP

In light of the available data on many synthetic and natural peptides that form ionic channels, we assumed a four-helix bundle conformation for SCP and treated each of the four transmembrane segments as adopting the α-helix structure. The optimal side-chain conformations of an isolated helical segment in SCP were calculated with neutral Asp and Glu residues, assuming that the charge at the ionized residues would be compensated by counter-ions. At the starting point of the MCM trajectory, the main chain torsions were assigned α-helical values and the side-chain torsions were assigned values optimal for the α-helical conformations of the corresponding model peptides: *N*-acetyl-X-*N*-methylamide (X = amino acid). The conformational properties of the model peptides calculated using the ZMM package were very similar to those reported by Vasquez et al. (1983) (Zhorov, unpublished data). In the subsequent starting points, the side-chain torsions were randomly sampled and the energy was minimized with both side-chain and main-chain torsions varied. If during energy minimization the α-helical conformation of the main chain was disrupted, the corresponding point was not accepted into the trajectory. In the lowest energy MEC, the isolated transmembrane segment of SCP had an α-helical structure slightly bent at the level of Gly-13. In further calculations of the channel peptide, main-chain torsions of the four transmembrane segments from Pro-2 to Glu-22 were fixed in the above conformation. The β-hairpin initial conformation was used for the template nanopeptide, as suggested by Grove et al. (1991).

The four-helix bundle topology

The helical structure of the transmembrane segments was imposed by fixing the backbone torsional angles. Geometrical restraints were then used to create different models of the SCP interacting with Ca^{2+} ions and nifedipine. The energetically optimal models were verified later without restraints. Two types of the restraints were used. The restraints of the first type imposed the ionizable acidic residues to face the pore. These residues are the evident candidates to interact with the permeating Ca^{2+} ions inside the pore, whereas their contacts with the lipid bilayer would be unfavorable. An α-helical wheel representation of the transmembrane segment (Fig. 3) showed residues Asp-7, Asp-17, and Glu-22 falling in a relatively short arc with the C^{β} atom of Trp-3 residue approximately representing the center of the arc. The distances between the C^{β} atoms of Trp-3 residue in the diagonally spaced helices were restrained within the boundaries of 9–11 Å. The minimal number of the restraints and their relatively wide boundaries helped compromise the intrapore orientation of the acidic residues with interactions opposing this orientation.

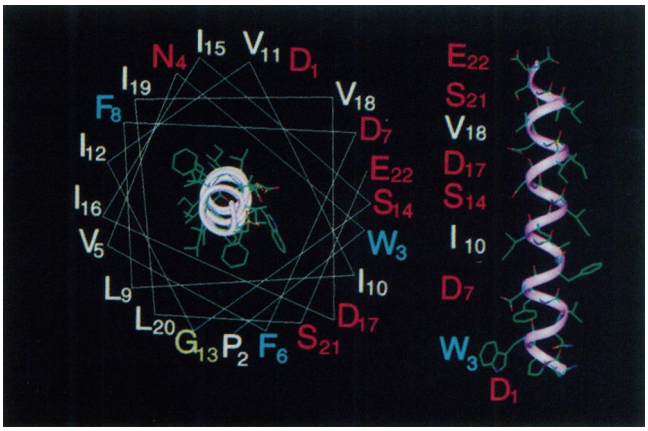

FIGURE 3 Top and side views of one of the α-helical transmembrane segments of SCP (the side-chain conformations correspond to those found in the MEC P1; see text). The polar, hydrophobic, aromatic, and Gly-14 residues are shown, respectively, in red, white, blue, and light green. In the α-helical wheel diagram superimposed over the top view (*left*), the residue designations are positioned at the extensions of the lines drawn from the helix axis via the corresponding side chains. Polar residues are grouped in the hydrophilic 90° sector and constitute a pathway for Ca^{2+} permeation. The hydrophilic sector is also faced by the hydrophobic residues Ile-10 and Val-18. The remaining 270° sector is hydrophobic with only one hydrophilic residue, Asn-4. The residue Asp-1 following the helix-braking residue Pro-2 is not considered a part of the α-helical structure. Note that C^{β} atom of the Trp-3 residue is approximately in the middle of the hydrophilic sector.

Interaction of SCP with Ca^{2+} ions: the zero-net-charge model

The SCP incorporates 24 ionizable groups: 16 acidic residues, four basic groups (N-termini) in the transmembrane segments, and four ionizable groups in the nanopeptide template (Lys-2, -Glu-7, N-, and C-termini). Because the ionizable groups in the template as well as in the N-termini of the transmembrane segments are common for both DHP-sensitive and non-DHP-sensitive peptides (Grove et al., 1993), they are not expected to be involved in interactions with the ligand. Therefore, these groups were treated as neutral, implying that their charges will be compensated by the counter-ions of the extra- and intracellular environment. The acidic groups in the transmembrane fragments that may directly interact with the permeating Ca^{2+} were considered in their ionized forms. Evidently at least some of the negative charges of these groups should be compensated by the permeating cations. The number of Ca^{2+} ions in the pore is

not known. We assumed that the pore incorporates eight Ca^{2+} ions, which would make the system electrically neutral (the zero-net-charge model).

The zero-net-charge model is less arbitrary than models with non-ionized or partially ionized acidic residues, because the mutual compensation of the positive and negative charges in a macromolecule and its immediate environment is energetically the most favorable situation. Alternative models would require additional assumptions of either a low pH inside the pore or the compensation of the charges at the ionized residues by implicit counter-ions. Both assumptions are weak: at physiological (millimolar) concentration of Ca^{2+} in the extracellular solution, pH inside the Ca^{2+} channel pore should be higher than in the bulk solution (see below), and the explicit consideration of Ca^{2+} ions, the natural occupants of Ca^{2+} channels, is more realistic than implicit consideration of nonspecified counter-ions. The accurate calculation of ion-ion interactions by the molecular mechanics method is problematic. Because ion-ion interactions in the zero-net-charge model would compensate each other, the calculations of this model would be more accurate than calculations of non-zero-net-charge models. Even if the real number of Ca^{2+} ions simultaneously bound to SCP is less than eight, the zero-net-charge model may be considered as a snapshot obtained with an exposure time of the few microseconds necessary for the permeation of a few Ca^{2+} ions. In such a snapshot, all of the potential binding sites for Ca^{2+} would be occupied. A last and important argument in favor of the zero-net-charge model is that it explains the electrophysiological and pharmacological properties of SCP, as will be shown subsequently.

Salt bridges between Ca^{2+} ions and SCP

Electrostatic interactions should maximize the number of salt bridges involving Ca^{2+} and any two of the acidic residues of the SCP. Because the number and mobility of water molecules inside the narrow four-helix bundle pore are limited, such bridges should be relatively stable. The four-helix bundle topology limits the number of the possible salt bridges. The C^{β} atoms of Asp-17 and Asp-7 in the same helix are separated by 16.2 Å, which excludes intrahelical salt bridges between levels B and C (Fig. 1). Interhelical salt bridges B-C as well as any salt bridges A-C, A-D, B-D would be even longer and, hence, are also excluded. The C^{β} atoms of Glu-22 and Asp-17 within a given helix are separated by 9.5 Å, permitting the formation of salt bridges between levels A and B. The bridges A-A, A-B, and B-B may be represented by patterns connecting eight vertices of a parallelepiped by four noncrossing lines; crossing lines would correspond to the bridges with two Ca^{2+} ions in nonrealistically close proximity. Patterns with the diagonal lines running through the pore axis would interfere with the intrapore binding of DHP ligand. This leaves eight primary patterns of salt bridges (Fig. 4). A number of symmetrical patterns may be obtained by rotating the primary patterns

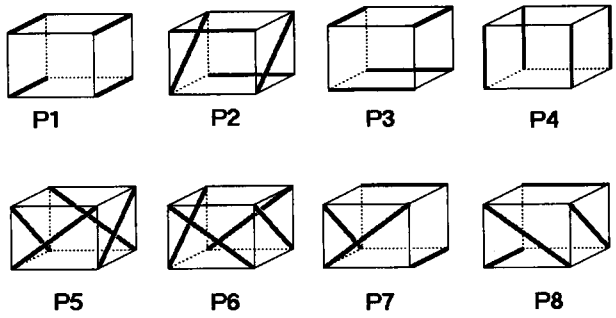

FIGURE 4 Eight conceivable patterns of salt bridges between Ca^{2+} ions and pairs of acidic residues of SCP. The top and bottom planes of the parallelepipeds represent levels A and B of the four-helix bundle, respectively (see Fig. 1). The vertical ribs of the parallelepipeds represent the helices H1 to H4 (shown anticlockwise from top right). The thick lines indicate the salt bridges.

around the vertical axis by 90°, 180°, or 270°. Because the helices are homologous, their rotation around the template-helix chains would accomplish the same helix-helix interactions in a primary pattern and in the patterns symmetric to it. The nanopeptide template would have different orientations relative to the salt bridges in the primary and symmetric patterns. However, the backbone of the template is remote from the salt bridges and should not strongly affect their stability. The above reasoning led us to consider the primary patterns only.

At level D, Asp-1 residues terminate the transmembrane segments following the helix-braking Pro-2 residues. Therefore, the main-chain conformation of Asp-1 is indefinite (the torsion angles ψ in Asp-1 residues were sampled in MCM trajectories; see Materials and Methods). In spite of the conformational flexibility of Asp-1 residues, salt bridges between levels C and D are not possible: inside the pore they would be sterically hindered by the bulky Trp-3 residues, and outside the pore they would expose Ca^{2+} to the lipid environment. Thus, Asp-7 and Asp-1 residues may be involved in intralevel bridges only. Because the intracellular water environment would destabilize electrostatic interactions between Ca^{2+} and Asp-1 residues, these interactions seem to be more important for "delivering" Ca^{2+} from the pore into the cell rather than for the stabilization of the SCP conformations. Therefore, no restraints between Asp-1 residues and Ca^{2+} ions were imposed. At level C, only two salt bridges may be formed simultaneously, half the number at the levels A-B. Hence, the bridges at level C would be less important in stabilizing the conformations of the channel. No restraints between Asp-7 residues and Ca^{2+} ions were therefore imposed, implying that the formation of the salt bridges at level C would comply with the salt bridges imposed by the restraints at levels A and B. In the starting conformation of each MCM trajectory, a pair of Ca^{2+} ions were placed in the vicinity of the carboxylate groups at both levels C and D. The locations of these ions were optimized during the MCM calculations.

Optimal conformation of the complex of SCP with Ca^{2+} ions

The eight primary patterns specifying salt bridges at levels A and B were evaluated in the eight restrained MCM trajectories (Table 1). The final (lowest) MECs found in the trajectories are designated by the names of the corresponding patterns (e.g., P1 in Fig. 4). The restraints specifying salt bridges were met in almost all of the final MECs. An exception was found in the MEC P6, in which some of the restrained distances for Ca^{2+}-O were 4–5 Å, exceeding the set limit by 1–2 Å (see Materials and Methods). Hence, pattern P6 is not consistent with the four-helix bundle topology of the SCP. The high energies of the MECs P2, P4, P6, P7, and P8 indicate poor consistency of the corresponding patterns with the four-helix bundle topology of the SCP. The MECs P1 and P3 are energetically much more preferable than other MECs. These two MECs are essentially different: MEC P1 corresponds to a wide pore, with room for a number of water molecules to neighbor each chelated Ca^{2+} ion, whereas the helices in the MEC P3 are tightly packed (Fig. 5). Between the two low-energy MECs P1 and P3 we chose the former, as it corresponded to a structure of SCP that would allow Ca^{2+} ions to permeate through and accommodate intrapore binding of DHP ligand as well. The structure P3 may represent one of the closed conformations of SCP. The capacity of the pore to adopt essentially different conformations may be the basis for one of the mechanisms of SCP gating in the absence of ligands. The crucial role of Ca^{2+} in stabilizing these MECs is consistent with the known Ca^{2+} requirement for selectivity and gating of ion channels (Armstrong and Miller, 1990).

In MEC P1, practically all polar residues of the channel are inside the pore, whereas the exterior is hydrophobic. Six Ca^{2+} ions bridge the helices H1-H4 and H2-H3 at the three levels (Fig. 6). Although only one atom in each of the eight acidic residues at the levels A and B was restrained to Ca^{2+} ion in the initial conformation, additional coordinating bonds appeared in the subsequent MCM trajectory. Thus, at level A, one pair of glutamates chelated the first Ca^{2+} ion tetradentately and the other pair of glutamates chelated the second Ca^{2+} tridentately. At level B, two aspartates chelated each Ca^{2+} ion tridentately. At level C, both Ca^{2+} ions were chelated tetradentately by two aspartates. At level D, salt bridges were not formed, and both Ca^{2+} ions were bound to single aspartates. Thus, in MEC P1, Ca^{2+} ions were organized in two files situated at diametrically opposite sides of the pore.

TABLE 1 MCM trajectories of Ca^{2+}-bound SCP calculated with restraints*

Salt bridge pattern‡	No. of energy minimizations	Lowest MEC		
		Step§	E,‖ kcal/mol	E_r,¶ kcal/mol
P1	7463	898	0	<1
P2	3515	2919	315	<1
P3	5400	3937	29	<1
P4	5000	4650	743	50
P5	5122	4481	117	<1
P6	900	900	3231	1986
P7	2900	2881	182	<1
P8	5700	5426	355	<1

*Ca^{2+}-O and Trp-Trp restraints; see text.
‡The patterns are designated as in Fig. 2.
§The number of energy minimization yielding the lowest MEC.
‖Above the lowest MEC P1 (the absolute energy of the MEC P1 is −1612 kcal/mol).
¶The energy of the restraints.

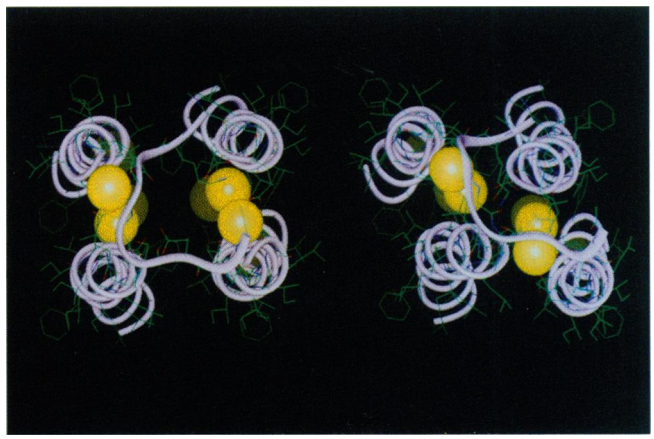

FIGURE 5 Lowest-energy MECs of SCP with eight Ca^{2+} ions found in the MCM trajectories with the restraints imposing the patterns of the salt bridges P1 (*left*) and P3 (see Fig. 4 for the sketches of the patterns P1 and P3 and Table 1 for their energies).

The α-helical wheel representation of one of the transmembrane segments of the channel in MEC P1 clearly demonstrates its amphipathic nature (Fig. 3). The acidic residues Asp-7, Asp-17, and Glu-22 face a 90° sector. Along with the hydrophilic residues Ser-21 and Ser-14, the acidic residues may constitute a path for the permeating Ca^{2+} ions. The aromatic residues Phe-6 and Trp-3, which face the hydrophilic sector, would also contribute their π-electrons for the interaction with the permeating Ca^{2+} ions. The remaining 270° sector of the wheel is hydrophobic, having only one hydrophilic residue, Asn-4.

Thus, formation of the salt bridges of the SCP with the permeating Ca^{2+} ions may sustain the 3-D structure of the pore lined up by the acidic residues. No calculations of the SCP without Ca^{2+} ions were performed. Such calculations would yield MECs with the acidic residues distanced from each other because of repulsion of their negative charges. It would be difficult to use such structures for the explanation of the electrophysiological and pharmacological properties of the SCP.

Asymmetry of Ca^{2+}-bound SCP

As was shown earlier, pairs of Asp-7, Asp-17, and Glu-22 residues in the adjacent helices of SCP sustain each file of Ca^{2+} ions. The C^{β} atom of Asp-17 (at level B) is most distanced from the median among C^{β} atoms of the three

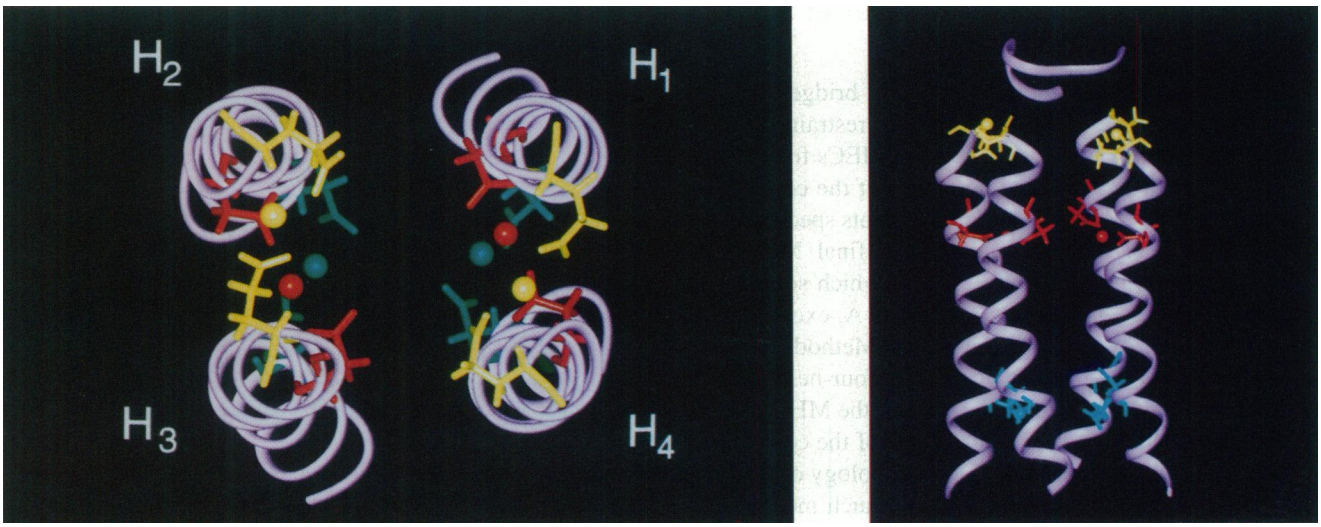

FIGURE 6 Top and side views of the SCP showing Ca^{2+} chelating patterns at the levels A (*yellow*), B (*red*), and C (*green*). At level A, one pair of glutamates chelate the first Ca^{2+} ion tetradentately, and the other pair of glutamates chelate the second Ca^{2+} tridentately. At level B, two aspartates (Asp-17) chelate each Ca^{2+} ion tridentately. At level C, both Ca^{2+} ions are chelated tetradentately. Note the asymmetric disposition of the acidic residues and Ca^{2+} ions relative to the pore axis. The asymmetry at level B (*red*) is the main cause of energy dissimilarity among different modes of nifedipine binding.

acidic residues in the same helix (Fig. 3). Asp-17 residues in the helices H1 and H3 are closer to the pore axis than Asp-17 residues in the helices H2 and H4 (Fig. 6). The side chains of the Asp-17 residues fold toward the pore axis to bring the carboxyl groups into the required proximity necessary to form the salt bridges. However, because the residues are relatively far from each other, their four oxygen atoms cannot reach the Ca^{2+} ion simultaneously and the ion is chelated only tridentately. Because each Asp-17 residue in the helices H1 and H3 offers a pair of oxygen atoms for interaction with Ca^{2+}, the cations are attracted closer to the helices H1 and H3 than to the helices H2 and H4. In the latter two helices, each Asp-17 residue offers only one oxygen atom for interaction with Ca^{2+}. A pair of Asp-17 residues chelating one ion cannot come any closer to each other by twisting the helices, because this would be resisted by the salt bridges at levels A and C. This asymmetry found in many MECs is, evidently, an intrinsic property of the SCP. The important consequence of this asymmetry is the energetic dissimilarity of different modes of nifedipine binding (see below).

Mechanism of Ca^{2+} influx and ion selectivity of the SCP

The arrangements of Ca^{2+} ions and the acidic residues at levels A, B, and C have a remarkable common feature: two Ca^{2+} ions are chelated by the carboxylate groups at the diametrically opposites sides of the pore, the center of the positive charge of each Ca^{2+} ion being closer to the pore axis than the centers of the negative charges at any of the carboxylate groups (Fig. 6). This arrangement has three important consequences. First, mono- or divalent cations trying to pass between the two chelated Ca^{2+} ions would meet the repulsion from their positive charges, which would prevail over the attraction by the negative charges of the carboxylate groups. Monovalent cations at physiological concentrations could enter the pore and, in principle, satisfy all of the negative charges. However, two monovalent cations have to collide simultaneously with Ca^{2+} to displace it. Because the probability of such a collision is low, monovalent cations have only a low chance of substituting the chelated Ca^{2+}. Contrarily, a divalent cation approaching the pore from the extracellular space may substitute any of the two Ca^{2+} ions chelated at level A and push it down the pore because of charge repulsion. This explains the Ca^{2+} selectivity of the SCP observed in experiments (Grove et al., 1993). Second, the repulsion between the two Ca^{2+} ions chelated at the same level of the pore is only minimally screened by the carboxylates. This repulsion would promote Ca^{2+} dissociation from the glutamates, thus facilitating Ca^{2+} permeation along the pore by a relay mechanism. (Water molecules in the pore would also facilitate Ca^{2+} movement between the binding sites by lowering the energy barriers between them due to formation of hydration shells (Hille, 1992). Third, electrically neutral drugs such as DHPs may fit the vacant space between the chelated Ca^{2+} ions and interact electrostatically with them. This provides for the possibility of a ternary association between SCP, Ca^{2+} and SCP ligands.

The above mechanism preventing monovalent cations to enter the pore applies also to the hydroxonium ion, the carrier of protons. Therefore, the local pH inside the pore should be higher than in the extra- and intracellular solutions implying that the acidic residues (at least at the levels A, B and C) should be permanently ionized. The ionized acidic residues would attract Ca^{2+} ions abundant in the extracellular space and in the vicinity of the pore. All these

considerations strongly support the present model in which Ca^{2+} ions neutralize the charges of the ionized acidic residues in the pore.

In the absence of Ca^{2+} ions in the extra- and intracellular bulk solutions, the cation binding sites in the SCP would be occupied by the monovalent cations. The electrostatic attraction of the monovalent cations to the acidic residues of the pore would not, however, be as strong as the attraction of divalent cations. This would explain the fact that in the absence of divalent cations, SCP has high permeability to monovalent cations (Grove et al., 1993).

"Gate" of the SCP

The difference in the dimensions of the pore in the conformations P1 and P3 (Fig. 5) may account for SCP gating in the absence of the ligand. Gating was also demonstrated for the ligand-bound SCP (Grove et al., 1991). The closed pore P3 would not accommodate the ligand. Because the lifetime of the ligand-SCP complex would exceed the lifetimes of individual open and closed states, there should be additional mechanisms of SCP gating in the P1 conformation. We explored this point by considering the hydrated Ca^{2+} ion.

It is well known that Ca^{2+} in bulk solution strongly interacts with water molecules of the first hydration shell. A possible pattern of Ca^{2+} coordination by water molecules was found in the crystal $CaBr_2 \cdot 10H_2O \cdot 2(CH_2)_6N_4$, where six water molecules lie around the Ca^{2+} at distances ranging from 2.32 to 2.35 Å (Hille, 1992). We assume that when Ca^{2+} enters the pore, at least six water molecules would accompany the ion. Some of the water molecules may be substituted by the hydrophilic groups inside the pore. In addition to the acidic residues Glu-22, Asp-17, and Asp-7, which face the pore and provide binding sites for Ca^{2+}, the pore is lined up by the hydrophilic residues Ser-21 and Ser-14, which may serve as the intermediate binding sites for Ca^{2+} ions permeating the pore (Fig. 3).

A loss of even one water molecule from the entourage of the permeating Ca^{2+} ion without compensation by an oxygen atom or π-electrons would be energetically unfavorable (Hille, 1992). Therefore, in the open channel, the pore at the levels of all the hydrophobic residues should be wide enough to accommodate Ca^{2+} with its entire water entourage. The narrowing of the pore even at one level of the hydrophobic residues would hinder the ion's passage, implying that the corresponding residues may represent the closed "gate" of the channel. Each transmembrane segment incorporates four hydrophobic residues that face or may face the pore: Val-18, Ile-10, Phe-6, and Trp-3 (Fig. 3). Trp-3 and Phe-6 residues should not be a decisive obstacle to Ca^{2+} permeation because their π-electrons would at least partially substitute the water molecules in the entourage of Ca^{2+}. This suggestion is supported by the fact that mutations of Leu-577 to Trp in the pore-forming M2 transmembrane segment of the glutamate receptor increased the permeability of the channel to divalent cations by three to four times (Ferrer-Montiel et al., 1995). The pore at the level of Val-18 is wide enough to accommodate the $Ca^{2+}:(H_2O)_6$ complex. Thus, a bracelet of four Ile-10 residues remains the only candidate to serve the role of the hydrophobic "gate" in SCP.

The minimal-profile projection of the complex $Ca^{2+}:(H_2O)_6$ may serve as a rough criterion to discriminate the open and closed states of the pore at the levels of hydrophobic residues. To obtain such a projection, we calculated a 1000-step MCM trajectory of the cluster $Ca^{2+}:(H_2O)_6$ in vacuo. It yielded the apparent global MEC with the six water molecules H-bonded to each other at one side of the Ca^{2+} sphere (see Fig. 7). The dimensions of the minimal-profile rectangle (Voitenco et al., 1991) described over the apparent global MEC of the cluster $Ca^{2+}:(H_2O)_6$ are 5.5 × 7.9 Å. Interestingly, the dimension of the shorter side of the rectangle (5.5 Å) is close to the "diameter" of $N(CH_3)_4^+$ (about 6 Å), the largest organic cation permeable through the L-type Ca^{2+} channel (McCleskey and Almers, 1985).

Fig. 7 shows the bracelet of four Ile-10 residues in two different conformations found among the MECs accumulated in the MCM trajectory P1. In both conformations, the profile of the pore between the four Ile-10 residues is roughly congruent to the minimal-profile projection of the cluster $Ca^{2+}:(H_2O)_6$. The cluster fits better in one MEC than in the other. In both MECs, the pore at the level of Ile-10 residues is not wide enough to let the cluster $Ca^{2+}:(H_2O)_6$ pass through. However, the dynamic oscillations of the channel and the cluster may help the latter to pass; the probability of passing via the wider MEC is, evidently, higher. This supports the suggestion that the bracelet of Ile-10 residues may represent the gate of the SCP. The two

FIGURE 7 Ring of four Ile-10 residues representing the "gate" of the SCP in the closed (*left*) and open (*right*) conformations found in MCM simulations (see text). The helices H1 to H4 are shown anticlockwise from top right. The energetically optimal conformation of the cluster $Ca^{2+}:(H_2O)_6$ (see text) fits the open gate better than the closed gate: in contrast to the open conformation, the methyl group of H1 Ile-10 residue (shown in *light blue*) in the closed conformation protrudes into the pore, pushing the cluster from H4 Ile-10 toward H3 Ile-10 residue. The permeation of Ca^{2+} via the closed gate would require energetically unfavorable separation of at least one water from the entourage of the cation.

MECs transform to each other by rotation of one Ile-10 residue rather than by the movement of the helices. The lifetimes of the open and closed states of the SCP are in milliseconds (Grove et al., 1993), implying that the barrier height between the two states is about 12 kcal/mol. The barrier for nonhindered rotation around a C-C bond (about 3 kcal/mol) provides nanosecond lifetimes of the conformations. However, in the optimal conformation of the SCP, Ile-10 residues of the helices H1 and H2 are in close contact with those in the helices H4 and H3, respectively (Fig. 7). These contacts hinder the rotation of Ile-10 residues and would increase the lifetimes of their conformations to the level compatible with the lifetimes of the open and closed states of the channel. However, accurate calculation of the rotational barriers for Ile-10 residues in a model of SCP with rigid valence geometry is problematic. So, we do not exclude the possibility that movements of the helices not observable in the MCM simulations may determine the lifetimes of the open and closed states. But, even in this case, the direct interaction of the ligand with the "gate" (see below) may modulate the stability of their conformations and hence the probability of the open and closed states.

Structure of SCP with bound nifedipine ligand

Bioactive conformation of nifedipine

The structural formulae of the DHP ligands active at SCP are shown in Fig. 8. The probable conformation of nifedipine prevailing at the receptor site of an L-type Ca^{2+} channel is a flattened-boat DHP ring orthogonal to the plane of a pseudoaxial 4-aryl group at the "bowsprit" with the polar group in the bowsprit maximally separated from the NH group at the stern (Goldmann and Stoltefuss, 1991; Govyrin and Zhorov, 1994). The substituents at the starboard and port sides of the DHP ring are flexible and may be involved in Ca^{2+} binding, as was predicted by Zhorov and Govyrin (1985) and was shown experimentally for nicardipine by Belciug and Ananthanarayanan (1994). We have assumed that the above conformation would prevail for nifedipine in the pore of SCP. In this conformation, nifedipine has an overall elongated shape, with the long axis passing via extended carbomethoxy groups (Fig. 9). Three orientations of the conformer inside the pore are possible: 1) 4-aryl plane normal to the pore axis, 2) the plane of the DHP ring normal to the pore axis, and 3) both DHP ring and 4-aryl planes parallel to the pore axis. The dimensions of the minimal-profile rectangles (Voitenco et al., 1991) described over a wire-frame model of nifedipine (Fig. 9) show that the latter would fit a pore as small as 6.2 × 8.6 Å in the first binding orientation, whereas the second and the third orientations would require pore sizes of 8.6 × 11.4 and 6.2 × 11.4 Å, respectively (taking into account van der Waals radii of atoms along the sides of the rectangles, the actual dimensions of the pore should be 2.4–2.6 Å larger). The narrow pore of the four-helix bundle is likely to accommodate nifedipine bound in the first orientation only, and hence further calculations were made using this orientation of the drug.

Starting conformations for nifedipine docking

The energies of possible complexes of nifedipine with SCP were obtained by calculating MCM trajectories. Only local conformational changes in the SCP and nifedipine were expected during one MCM trajectory. Larger changes such as flip-flop of the ligand in the pore, rotation of nifedipine along its long axis, and translation of nifedipine along the pore would have small probability of being accepted in the MCM trajectory because such changes would involve relatively high energies for the MECs (see Materials and Methods). Therefore, different starting conformations were chosen to explore distinctive sites and modes of nifedipine binding. The pore beneath levels A and B is faced, respectively, by the relatively small Ser-21 and Ser-14 residues,

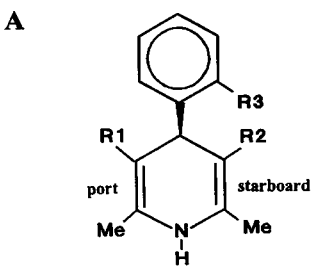

Compound	R1 port	R2 starboard	R3	Effect
Nifedipine	COOMe	COOMe	NO_2	Blocker
(R)-Bay K 8644	COOMe	NO_2	CF_3	Blocker
(S)-Bay K 8644	NO_2	COOMe	CF_3	Activator

FIGURE 8 (*A*) Structural formulae of the dihydropyridine ligands nifedipine, (*R*)-Bay K 8644 and (*S*)-Bay K 8644. (*B*) Sketch of the bioactive conformation of nifedipine. Indicated are the starboard and port sides of the DHP ring.

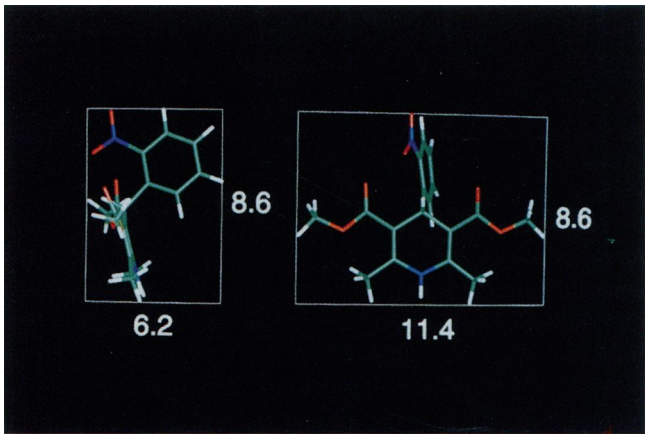

FIGURE 9 Bioactive conformation of nifedipine projected at the plane parallel to the 4-aryl group (*left*) and at the plane parallel to the DHP ring (*right*). The dimensions (in angstroms) of the minimal-profile rectangles described over the projections are shown. The dimensions of the projection at the plane perpendicular to both the DHP and 4-aryl rings (not shown) are 6.2 × 11.4 Å. Taking into account van der Waals radii of the hydrogen (1.2 Å) and oxygen (1.4 Å) atoms located against the sides of the rectangles, the dimensions of the rectangular pores to accommodate the MECs should be 8.8 × 11.2 Å, 11.2 × 13.8 Å, and 8.8 × 13.8 Å, respectively, for the three projections.

whereas the pore between levels C and D is crowded by the bulky aromatic residues. Therefore, the sites between levels A and B (level A-B) and between levels B and C (level B-C) were considered most promising for the docking experiments. At both sites, two chelated Ca^{2+} ions protrude into the pore. Only the shorter side of the elongated rectangle approximating the minimal profile of nifedipine (Fig. 9) may fit between Ca^{2+} ions. Two orientations of the rectangle are possible, with the bottom of the DHP ring facing the salt bridge between helices H2-H3 in one case and between helices H1-H4 in the other. In each orientation, two modes of nifedipine binding are possible, one where the port-side group points up and another where it points down the pore. The four types of nifedipine orientations at each of the levels A-B and B-C make eight possible binding combinations. Therefore, eight independent MCM trajectories were calculated.

A typical docking was simulated as follows. Using the graphical interface, nifedipine was placed at a specific level. The number of bad contacts (overlaps) between the ligand and the channel was minimized initially by manual adjustments of the ligand. However, it was not possible to remove all of the bad contacts. Because these contacts could cause the separation of the helices during minimization, the first stage of the MCM trajectory was calculated with the restraints between diagonally spaced Trp-3 residues. The restraints were then removed and the second stage of the MCM trajectory was carried out.

Complexes of SCP with DHPs

The energies of the lowest MECs found in each trajectory are given in Table 2. At the level A-B, a few of the functional groups of the channel were involved in the binding and two Ca^{2+} ions were chelated simultaneously by nifedipine (Fig. 10). However, the bulky Val-18 residues that partially protrude into the pore caused the ligand binding at this level to be energetically unfavorable. Nifedipine binding at the level B-C was more preferable, even though fewer ligand-channel hydrogen bonds occurred here. The NH group of nifedipine, important in binding to L-type channels (Goldmann and Stoltefuss, 1991), was remote from any proton-acceptor group in the most optimal MEC

TABLE 2 MCM simulations of nifedipine docking to SCP*

Ligand binding mode				Lowest MEC		Ligand contacts§					
Level	Port-side direction	DHP bottom direction	No. of energy minimizations	Step when it appeared	Energy, kcal/mol‡	$=O_p$	$>O_p$	$=O_s$	NO′	NO″	NH
I. Binding inside the pore											
A–B	Up	H1–H4	3697	2757	57	Ca^{2+}		Ca^{2+}	Ca^{2+}‖		1S21
A–B	Up	H2–H3	2409	1605	59			Ca^{2+}			3S21‖
A–B	Down	H1–H4	3142	2582	63				1S21		
A–B	Down	H2–H3	8759	6561	97		1S21‖	Ca^{2+}			4E22‖
B–C	Up	H1–H4	6604	4650	17			4S14	Ca^{2+}	4S14‖	2S14‖
B–C	Up	H2–H3	6100	5493	37				Ca^{2+}		4S14‖
B–C	Down	H1–H4	9300	5508	26	2S14‖		Ca^{2+}			3D17
B–C	Down	H2–H3	14000	13546¶	0			Ca^{2+}			
II. Binding outside the pore											
B	Down	H2–H3	16300	13952	9						

*The trajectories started from the lowest MECs obtained in the preceding MCM trajectories calculated with Trp-Trp restraints.
‡Relative to the lowest MEC found in all the trajectories (the absolute energy of the lowest MEC is −1665 kcal/mol).
§Ca^{2+} ions or SCP groups forming donor-acceptor contacts with the ligand. The subscripts p and s designate port and starboard side-chain groups of nifedipine, respectively. The prefix before the SCP residue designation stands for the helix number (see Fig. 1).
‖Donor-acceptor contacts are possible via water molecule (the distance between donor-acceptor atoms are 3–4 Å).
¶The energy reached −1660 kcal/mol (below levels found in any other trajectory) at the 2245th energy minimization.

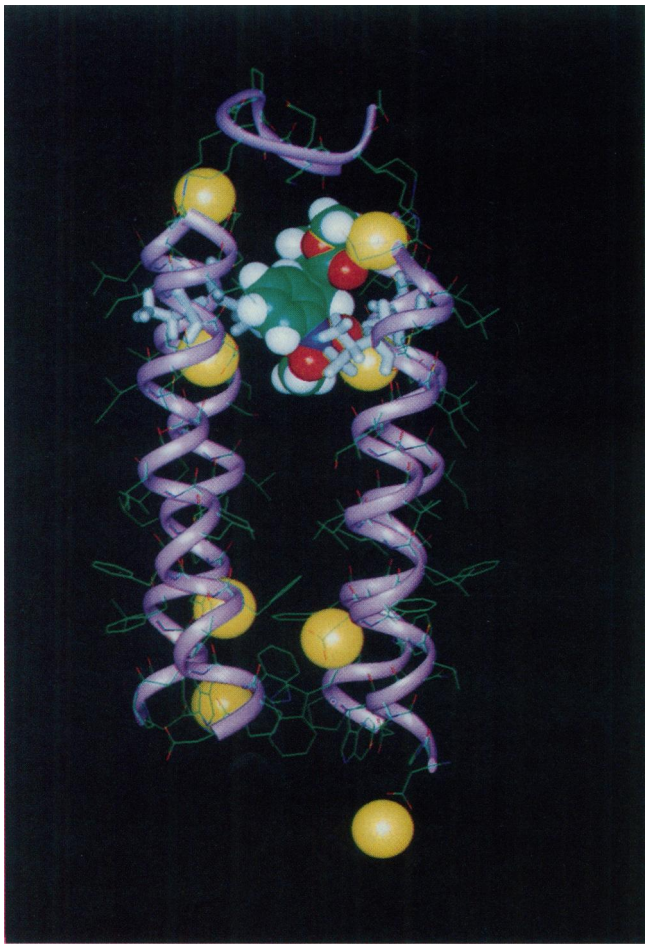

FIGURE 10 SCP with nifedipine bound at the level A-B with the port-side group pointed up the pore and the bottom of the DHP ring pointed to the helices H1-H4. Although the ligand coordinates two Ca^{2+} ions, the complex is energetically unfavorable because of repulsion of the ligand from Val-18 residues (*light blue*).

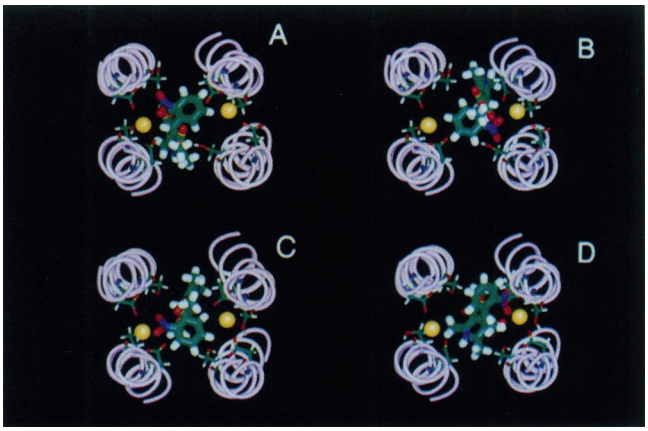

FIGURE 11 Top view of the four modes of nifedipine binding to SCP at the level B-C. In each mode, helices H1 to H4 are shown anticlockwise from the top right. (*A*) Nifedipine port-side group points in the extracellular direction (up the pore), and the bottom of the DHP ring points between the helices H2-H3. (*B*) Nifedipine port-side group points up the pore, and the bottom of the DHP ring points between the helices H1-H4. (*C*) Nifedipine port-side group points down and the pore and bottom of the DHP ring points between the helices H2-H3. (*D*) Nifedipine port-side group points down the pore, and the bottom of the DHP ring points between the helices H1-H4. The energies of the four binding modes are given in Table 2. Only Ser-14 and Asp-17 residues that may have donor-acceptor interactions with the ligand either directly or via Ca^{2+} ions or water molecules are shown. Note that Ca^{2+} ions are located more closely to the helices H1 and H3 than to the helices H2 and H4. This asymmetry may account for the fact that the port-down modes of nifedipine binding are more preferable energetically than the port-up modes (see text).

of SCP-nifedipine complex (Table 2). It should be emphasized that the present model does not consider water molecules, which should fill the pore. Some of these molecules may provide additional H-bonds for nifedipine binding. It is important to note, however, that the most significant contribution to binding energy comes from the ligand-Ca^{2+} interaction inside the pore rather than from other weaker noncovalent interactions.

Ligand binding with the port-side group pointing down the pore and the bowsprit polar group pointing to the Ca^{2+}-bridged helices H2-H3 at the level B-C turned out to be most preferable energetically (Fig. 11 *C*). This is in conformity with the asymmetry of the SCP described earlier. In the less favorable port-side-up modes of nifedipine binding, the NO_2 group of the ligand approaches Ca^{2+} from the side of the more remote helix, pushing the bulky DHP ring into a less spacious half of the pore interior. This difference in the port-up and port-down modes of binding is crucial to explaining the opposite effects of the (*R*)- and (*S*)-enantiomers of Bay K 8644, as will be shown below.

In the energetically preferable mode of binding, nifedipine fits snugly into the pore, as evidenced by the fact that, after removing the ligand, MCM simulation of the pore results in only minor changes of the side-chain conformations. The complex is stabilized by Ca^{2+} ion bound between two Asp-17 residues and the hydrophilic group of the ligand (Fig. 12). The latter could substitute water molecules adjacent to Ca^{2+} in the ligand-free pore and thus would not obstruct Ca^{2+} movement along these hydrophilic groups. The level of the pore critical for Ca^{2+} permeation is at the interface between DHP and the "gate" of SCP. The chemical structure of the DHP group abutting the gate may thus control the ion permeation (see below).

A few other MCM trajectories were calculated to estimate the relative stability of the optimal structure. Translation of nifedipine in the membrane plane 30 Å from the pore axis yielded a structure with an energy of 60 kcal/mol above the lowest MEC found in the trajectories (the "best" MEC). This demonstrates that binding of nifedipine to the four-helix bundle is energetically preferable. Another MCM trajectory started from a structure with nifedipine bound outside the pore and yielded an optimal structure with the CH_3, NH, and C=O groups of the ligand deeply penetrating the interface between helices H2-H3 and the C=O group approaching the intrapore-bound Ca^{2+}. However, the energy of this conformation was 9 kcal/mol above the best MEC (Table 2), demonstrating that intrapore binding of the ligand

FIGURE 12 Top and side views of the SCP with nifedipine bound at the level B-C with its port-side residue pointed down the pore and the bottom of the DHP ring pointed to the helices H2-H3. The ligand's polar groups, which coordinate Ca^{2+}, would not hinder the passage of the ion via corresponding level of the pore compared to the ligand-free pore filled with water molecules. The level of the pore critical for Ca^{2+} permeation is at the interface between the DHP port-side group and the "gate" of Ile-10 residues (whose van der Waals spheres are shown in light blue). The methyl moiety in the port-side group of nifedipine approaches the "gate" and may stabilize its closed conformation.

is preferable to extrapore binding. Because our calculations ignore effects of environment, entropy, and other factors, the computed energy difference may not be useful for estimating the probabilities of intrapore versus extrapore binding. However, the calculations do demonstrate the sterical and energetic possibility of intrapore binding. A much stronger argument in favor of intrapore binding is that it explains structure-activity relationships of DHPs (see below).

An attempt to insert the ligand at level C failed as the ligand was pushed out of the pore. Space-filling displays of the optimal structure (Fig. 13) show that although the pore

FIGURE 13 Space-filling views of the synthetic calcium channel with nifedipine (shown in *purple*) in the optimal mode of binding. The pore is accessible for the ligand from the interface between the helices H1-H2 and H3-H4 exposed to the lipid bilayer but not accessible from either the top or the bottom openings of the channel.

is not accessible for nifedipine ligand from the sides exposed to extra- and intracellular solutions, it is accessible from the side exposed to the lipid bilayer. This indicates that the binding of nifedipine inside SCP is possible not only thermodynamically but also kinetically.

We also carried out simulations of the binding of (*R*)- and (*S*)-Bay K 8644 to SCP to illustrate the important difference between a blocker and an activator. In these calculations, the optimal mode of the nifedipine-SCP complex was used as the starting point. In the absence of parameters for the fluorine atom in the ECEPP/2 force field, hydrogen atoms were used to calculate van der Waals interaction of the fluorine atoms with other atoms. Because the CF_3 and NO_2 groups of Bay K 8644 are not larger than the corresponding substituents in nifedipine, the starting points of the trajectories had low energy. The trajectories converged rapidly, the ligands moving slightly to provide close contact between their CF_3 groups and Ca^{2+} (Fig. 14).

Possible mechanism of SCP gating modulation by DHPs

DHP ligands do not affect the amplitude of the Ca^{2+} current in SCP, but alter the open state probability (Grove et al., 1993). The passage via gate cannot be a rate-limiting step for Ca^{2+} permeation for the following reason. If the gate is open, water molecules would rearrange around Ca^{2+} to adopt a conformation congruent to the space between the Ile residues (lumen). Because such a rearrangement does not require separation of Ca^{2+} and water molecules, the energy barriers would be small (say, 3 kcal/mol) and the time for the rearrangement would be in nanoseconds. If the gate is closed, the cluster would have to shed a water molecule. This is costly (>15 kcal/mol; Hille, 1992), and the ion passage will require about a second. In reality, Ca^{2+} permeates SCP in microseconds (Grove et al., 1993). The barrier for this should only be about 7–8 kcal/mol. Cleavage

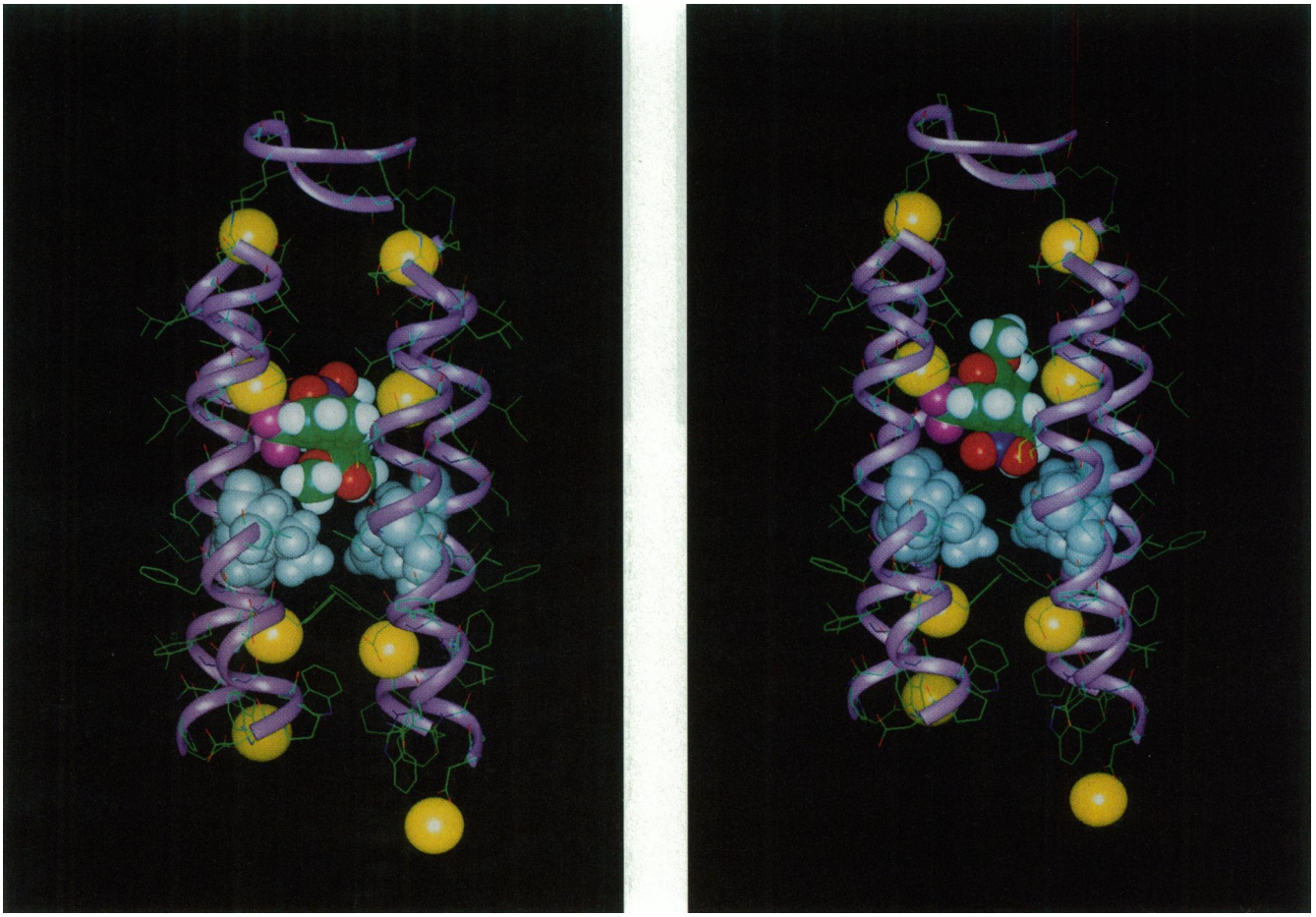

FIGURE 14 Side views of the SCP with the bound blocker (*R*)-Bay K 8644 (*left*) and activator (*S*)-Bay K 8644 (*right*). The (*R*)-isomer extends its hydrophobic port-side group to the "gate" and may stabilize its closed conformation. The (*S*)-isomer has only a short hydrophilic residue that does not plug the "gate" and hence stabilizes the open conformation of the pore (see text).

of bonds between Ca^{2+} and carboxylates (accompanied with their substitution by water molecules) may easily account for such a barrier. Because glutamates are longer and more flexible than aspartates, they would hold Ca^{2+} more tightly. Therefore, the dissociation from glutamates may be the rate-limiting step for the permeation.

Both blockers and activators bound inside the pore would stabilize its "wide-pore" conformation P1 and exclude the transition of SCP to the "flattened-pore" conformation P3, which is not permeable to hydrated Ca^{2+} ions (Fig. 5). However, this cannot explain the gating of the ligand-bound SCP observed by Grove et al. (1991). A basis for the gating may be the hindered rotation of Ile-10 residues, whose open and closed state probabilities may be modulated by the ligand group adjacent to them. In any of the four modes of binding at level B-C, the SCP blocker nifedipine exposes a hydrophobic side-chain group toward the Ile bracelet (Fig. 12). The latter would occlude the space between the Ile residues and stabilize the closed conformation of the gate due to Van der Waals and hydrophobic interactions. Interestingly, conformations with both open and closed gates (Fig. 7) were accumulated in MCM simulations of nonliganded channel as well as in the MCM simulations of nifedipine bound at level A-B inside and outside the pore. However, only conformations with the closed gate were found in a long MCM trajectory simulating nifedipine bound inside the pore between levels B-C.

Our model of SCP also accounts for the opposite effects of enantiomers of Bay K 8644, the (*R*)-enantiomer favoring the closed conformation and the (S)-enantiomer favoring the open conformation. According to the calculations, the port-down modes of nifedipine (and, possibly, other DHPs) binding are energetically preferable to the port-up modes (Table 2). The structural reason for this is the asymmetry of the Ca^{2+} chelation at level B of the SCP (see above). In the blocker (*R*)-Bay K 8644, the port-side group is the same as in nifedipine (Fig. 8). Favorable van der Waals interaction of this group with the bracelet of Ile-10 residues would stabilize its pore-closing conformation (Fig. 14 *a*). In the channel activator (*S*)-Bay K 8644, the port-side group is not long enough to reach the bracelet (Fig. 14 *b*). Therefore, the stabilization of the "wide-pore" conformation P1 would dominate in the action of the ligand. In addition, the closed conformation of the hydrophobic bracelet may be destabi-

lized by unfavorable contacts with water molecules adjacent to the activator's polar group NO_2. This would explain the intriguing paradox in the structure-activity relationships of DHPs. There are L-type Ca^{2+} channel activators with only CH_3 group as a port-side substituent or even without the substituent (Goldmann and Stoltefuss, 1991). Although the activity of such compounds at the SCP remains unknown, this mechanism would predict them to activate SCP.

On the functional analogy between SCP and L-type Ca^{2+} channels

The fact that the SCP composed of the four IVS3 segments of the L-type channel resembles the latter in its electrophysiological and pharmacological properties implies that the S3 segments may contribute to the pore lining (Grove et al., 1993). On the other hand, the pore of the voltage-gated ionic channels was postulated to be lined up by the short segments SS1-SS2 incorporating highly conserved residues (Guy and Conti, 1990), and subsequent experiments proved this prediction. For example, the mutation (K1422E) in the SS1-SS2 region of the sodium channel conferred on it certain properties of the Ca^{2+} channel (Heinemann et al., 1992). Site-directed mutations in the SS1-SS2 region of the L-type channel revealed four glutamate residues contributing to Ca^{2+} selectivity (Yang et al., 1993; Kim et al., 1993; Mikala et al., 1993). All of this strongly suggests that the SS1-SS2 segments line at least a part of the pore of L-type Ca^{2+} channels.

Grove et al. (1993) harmonized the two lines of evidence by suggesting that the SS1-SS2 segments are located at the entry of the pore of the L-type Ca^{2+} channel and modulate the ionic selectivity of a permeation pathway formed by a bundle of α-helical S3 transmembrane segments. Further experiments and molecular modeling studies are necessary to test this suggestion. Even if the S3 segments do not contribute to the pore of the L-type channel, the SCP may be considered as a model Ca^{2+} channel whose relatively simple and unambiguous chemical structure may help us to understand the basic principles of the ion selectivity and pharmacological sensitivity of the Ca^{2+} channels. Therefore, it is worthwhile to discuss some of the elementary properties of the L-type Ca^{2+} channel in view of the structural model of the SCP.

In the absence of the experimental data on the 3-D structure of the L-type Ca^{2+} channel, electrophysiological experiments are accounted for by phenomenological models that postulate a number of the binding sites for Ca^{2+} inside the pore, the distance between the sites, affinity of the sites for Ca^{2+}, etc. (see Tsien at al., 1987, for a review). The fundamental property of the authentic Ca^{2+} channels is their high selectivity for Ca^{2+} ions with millimolar Ca^{2+} in the bulk solution and a large permeability for monovalent cations when the concentration of divalent cations in the bulk solution is below the micromolar level (Kostyuk et al., 1983; Almers et al., 1984; Hess and Tsien, 1984). Intriguingly, the current of monovalent cations is blocked by micromolar Ca^{2+}, implying the presence of a high-affinity binding site for Ca^{2+}, whereas the observed Ca^{2+} current (0.1–1 pA) implies millimolar affinities for Ca^{2+} binding sites at the permeation pathway. Similar properties were demonstrated for the SCP (Grove et al., 1991, 1993). The above paradox was accounted for by two different models. Almers and McCleskey (1984) and Hess and Tsien (1984) postulated the presence of at least two high-affinity binding sites for Ca^{2+} inside the pore; at the micromolar Ca^{2+} in the bulk solution, one Ca^{2+} ion would occupy the first site "guarding" the pore from the monovalent cations; at millimolar Ca^{2+} in the bulk solution, both sites would be occupied by Ca^{2+} ions, their repulsion decreasing the apparent affinity for the binding sites to the millimolar range. An alternative model was proposed by Kostyuk et al. (1983). The authors postulated that Ca^{2+} channels exist in two different conformations, one selective for monovalent cations, the other for divalent cations; the occupation of a regulatory high-affinity Ca^{2+} site outside the pore would induce the conformational change. The latter phenomenological model may account for the same experiments, which back the multi-ion model (Mironov, 1992).

Our structural model of SCP explicitly presents the multi-ion pore. However, the mechanism of Ca^{2+} selectivity does not exactly correspond to the mechanism postulated for the multi-ion authentic Ca^{2+} channels. In the SCP, the neighboring Ca^{2+} binding sites are not extended along the pore. They are at the same levels normal to the pore axis. At low Ca^{2+} concentration in the bulk solution, one high-affinity complex would be formed between Ca^{2+} and two Glu-22 residues. The remaining two Glu-22 residues would also contribute to the energy of Ca^{2+} binding by long-range electrostatic interactions. This would explain the experimentally observed blockade of Na^+ current through SCP by micromolar Ca^{2+} (Grove et al., 1991). At millimolar Ca^{2+}, two salt bridges would be formed at the level of Glu-22. The dipole-dipole repulsion between the two salt bridges would decrease the affinity of Ca^{2+} ions to both of the sites, allowing fast permeation of Ca^{2+} ions through the pore. Similar events would occur at the levels of Asp-17 and Asp-7 residues, although the less flexible side chains of the Asp residues would provide a less perfect coordination of Ca^{2+} in comparison to Glu residues.

Both authentic and synthetic Ca^{2+} channels are similarly affected by DHPs and other ligands (Kokubun et al., 1986; Grove et al., 1991). Our calculations demonstrate that the asymmetry of the disposition of the Asp-17 residues relative to the pore axis is the main reason for the energy variation of different modes of DHP ligand binding and may account for the different effects of enantiomers of Bay K 8644. Interestingly, mutation experiments on L-type Ca^{2+} channels also reveal the functional asymmetry of the four Glu residues around the central pore (Yang et al., 1993; Kim et al., 1993; Mikala et al., 1993).

Recent experiments by Kuo and Hess (1993a,b) have presented new evidence for the multi-ion model of the Ca^{2+} channel. The authors postulated the presence of at least

three sets of the binding site for Ca^{2+}, including two closely spaced high-affinity sites. This agrees with our model. However, such arguments cannot prove that the S3 segments contribute to the pore lining in the L-type Ca^{2+} channel.

In summary, our results rationalize the Ca^{2+} selectivity of the SCP and its pharmacological sensitivity and account for the paradoxical fact that (*R*)- and (*S*)-enantiomers of Bay K 8644 have opposite effects on the probability of the channel open state. They demonstrate the crucial role of Ca^{2+} in the stabilization of the structure of SCP and DHP ligand binding. The amino acid sequences of the pore-forming elements of the authentic and synthetic Ca^{2+} channels are most probably different. However, the peculiarities of their 3-D structures relevant to Ca^{2+} permeation and DHP binding may be similar. Ca^{2+} ions would also function as the structure-forming elements of the L-type channel pore. DHP ligands would also form the ternary complex with Ca^{2+} inside the L-channel pore modulating the stability of the closed conformation of the adjacent hydrophobic gate (more precisely, those elements of the much more complex gate mechanism of the L-type channel, which regulate the lumen of the pore). Blockers such as (*R*)-Bay K 8644 would increase the stability, whereas activators such as (*S*)-Bay K 8644 would decrease it. A model of the DHP receptor of the L-type channel proposed earlier based on the considerations of conformation-activity relationships of only ligands and their complexes with Ca^{2+} also explained structure-activity relationships of different drugs as a consequence of their ternary association with Ca^{2+} inside the channel pore (Govyrin and Zhorov, 1994). The relatively simple structure of SCP provides several possibilities to experimentally test the model elaborated in the present work.

We thank the referees of this paper for their valuable suggestions.

This work was supported in part by the MRC and NSERC of Canada.

Note added in proof: In a recent study, Labarca et al. (1995) have reported the results of mutation experiments on the nicotinic acetylcholine receptor (nAChR) which show that channel gating is governed symmetrically and independently by the five conserved Leu-9 residues near the midpoint of the M2 transmembrane domain. In AchR and homologous receptors, these Leu residues occupy a "kink" in each of the five M2 helices and point toward the pore in the closed state of the channel. Channel opening causes the helices to rotate so that the Leu residues do not occlude the ion conduction pathway. Mutation of each Leu-9 by Ser in nAChR shifted the dose-response curve of the receptor to the left by ~10-fold, suggesting that contacts involving each of the five Leu residues play an important role in gating. The 10-fold difference translated to a free energy contribution per contact of ~1.4 kcal mol^{-1}. These observations are remarkably similar to our data on the Ile-gated channel in SCP and lend support to the usefulness of simple model systems.

REFERENCES

Abagyan, R., and P. Argos. 1992. Optimal protocol and trajectory visualization for conformational searches of peptides and proteins. *J. Mol. Biol.* 225:519–532.

Almers, W., and E. W. McCleskey. 1984. Non-selective conductance in calcium channels of frog muscle: calcium selectivity in a single-file pore. *J. Physiol.* 353:585–608.

Almers, W., E. W. McCleskey, and P. T. Palade. 1984. A non-selective cation conductance in frog muscle membrane blocked by micromolar external calcium ions. *J. Physiol.* 353:565–583.

Ananthanarayanan, V. S. 1991a. Peptide hormones, neurotransmitters, and drugs as Ca^{2+} ionophores: implication for signal transduction. *Biochem. Cell Biol.* 69:93–95.

Ananthanarayanan, V. S. 1991b. Binding and translocation of Ca^{2+} by calcium channel drugs. *In* Proteins: Structure, Dynamics and Design. V. Renugopalakrishnan, P. R. Carey, I. C. P. Smith, S. G. Huang, and A. C. Storer, editors. Escom, Leiden. 305–308.

Ananthanarayanan, V. S., L. B. Taylor, and S. Pirritano. 1992. Transport of Ca^{2+} by diltiazem across the lipid bilayer in model liposomes. *Biochem. Cell Biol.* 70:608–612.

Ananthanarayanan, V. S., S. Tetreault, and A. Saint-Jean. 1993. Interaction of calcium channel antagonists with calcium: spectroscopic and modelling studies on diltiazem and its Ca^{2+} complex. *J. Med. Chem.* 36: 1324–1332.

Armstrong, C. M., and C. Miller. 1990. Do voltage-dependent K^+ channels require Ca^{2+}? A critical test employing a heterologous expression system. *Proc. Natl. Acad. Sci. USA.* 87:7579–7582.

Belciug, M.-P., and V. S. Ananthanarayanan. 1994. Interaction of calcium channel antagonists with calcium: structural studies on nicardipine and its Ca^{2+} complex. *J. Med. Chem.* 37:4392–4399.

Brooks, C. L., B. M. Pettitt, and M. Karplus. 1985. Structural and energetic effects of truncating long ranged interactions in ionic polar fluids. *J. Chem. Phys.* 83:5897–5908.

Catterall, W. A., and J. Striessnig. 1992. Receptor sites for Ca^{2+} channel antagonists. *Trends Pharmacol. Sci.* 13:256–262.

Ferrer-Montiel, A. V., W. Sun, and M. Montal. 1995. Molecular design of a AMPA/KA receptor highly permeable to divalent cations. *Biophys. J.* 68:A149.

Flockerzi, V., H. Ocken, and F. Hoffmann. 1986. Purification of a functional receptor for calcium-channel blockers from rabbit skeletal muscle microsomes. *Eur. J. Biochem.* 161:217–229.

Glossman, H., and D. R. Ferry. 1983. Solubilization and partial purification of putative calcium channels labelled with [^{3}H]nimodipine. *Naunyn Schmiedebergs Arch. Pharmacol.* 323:279–291.

Goldmann, S., and J. Stoltefuss. 1991. 1,4-Dihydropyridines—effects of chirality and conformation on the calcium antagonist and calcium agonist activities. *Angew. Chem. Int. Ed. Engl.* 30:1559–1578.

Gould, R. J., K. M. M. Murphy, and S. H. Snyder. 1984. Tissue heterogeneity of calcium channel antagonists binding sites labelled by [^{3}H]nitrendipine. *Mol. Pharmacol.* 25:235–241.

Govyrin, V. A., and B. S. Zhorov. 1994. Ligand-Receptor Interactions in Molecular Physiology. Nauka, St. Petersburg. (in Russian).

Grove, A., J. M. Tomich, T. Iwamoto, and M. Montal. 1993. Design of a functional calcium channel protein: inferences about an ion channel-forming motif derived from the primary structure of voltage-gated calcium channels. *Protein Sci.* 2:1918–1930.

Grove, A., J. M. Tomich, and M. Montal. 1991. A molecular blueprint for the pore-forming structure of voltage-gated calcium channels. *Proc. Natl. Acad. Sci. USA.* 88:6418–6422.

Guy, H. R., and F. Conti. 1990. Pursuing the structure and function of voltage-gated channels. *Trends Neurosci.* 13:201–206.

Heinemann, S. H., H. Terlau, W. Stuhmer, K. Imoto, and S. Numa. 1992. Calcium channel characteristics conferred on the sodium channel by single mutations. *Nature.* 356:441–443.

Hess, P., and R. W. Tsien. 1984. Mechanism of ion permeation through calcium channels. *Nature.* 309:453–456.

Hille, B. 1992. Ionic Channels of Excitable Membranes, 2nd Ed. Sinauer Associates, Sunderland, MA. 261–290.

Kalasz, H., T. Watanabe, H. Yabana, K. Itagaki, K. Naito, H. Nakayama, A. Schwartz, and P. L. Vaghy. 1993. Identification of 1,4-dihydropyridine binding domains within the primary structure of the α_1-subunit of the skeletal muscle L-type calcium channel. *FEBS Lett.* 331:177–181.

Kass, R. S., J. P. Arena, and S. Chin. 1991. Block of L-type calcium channels by charged dihydropyridines. Sensitivity to side of application and calcium. *J. Gen. Physiol.* 98:63–75.

Kim, M.-S., T. Morii, L.-X. Sun, K. Imoto, and Y. Mori. 1993. Structural determinants of ion selectivity of brain calcium channels. *FEBS Lett.* 318:145–148.

Knaus, H. G., T. Moshammer, H. C. Kang, R. P. Haugland, and H. Glossmann. 1992. A unique fluorescent phenylalkylamine probe for L-type Ca^{2+} channels—coupling of phenylalkylamine receptors to Ca^{2+} and dihydropyridine binding-sites. *J. Biol. Chem.* 267:2179–2189.

Kokubun, S., B. Prod'hom, C. Becker, H. Porzig, and H. Reuter. 1986. Studies of Ca channels in intact cardiac cells: voltage dependent effects and cooperative interaction of dihydropyridine enantiomers. *Mol. Pharmacol.* 30:571–584.

Kostyuk, P. G., S. L. Mironov, and Ya. M. Shuba. 1983. Two ion-selecting filters in the calcium channel of the somatic membrane of the mollusc neurons. *J. Membr. Biol.* 76:83–93.

Kuo, C. C., and P. Hess. 1993a. Ion permeation through the L-type Ca^{2+} channel in rat phaeochromocytoma cells—2 sets of ion binding sites in the pore. *J. Physiol.* 466:629–655.

Kuo, C. C., and P. Hess. 1993b. Characterization of the high-affinity Ca^{2+} binding sites in the L-type Ca^{2+} channel pore in rat phaeochromocytoma cells. *J. Physiol.* 466:657–682.

Labarca, C., M. W. Nowak, H. Zhang, L. Tang, P. Deshpande, and H. A. Lester. 1995. Channel gating governed symmetrically by conserved leucine residues in the M2 domain of nicotinic receptors. *Nature.* 376: 514–516.

Langs, D. A., P. D. Strong, and D. J. Triggle. 1990. Receptor model for the molecular basis of tissue selectivity of 1,4-dihydropyridine calcium channel drugs. *J. Comput. Aided Mol. Des.* 4:215–230.

Li, Z., and H. A. Scheraga. 1988. Structure and free energy of complex thermodynamic systems. *J. Mol. Struct. (Theochem).* 179:333–352.

McCleskey, E. W., and W. Almers. 1985. The Ca channel in skeletal muscle is a large pore. *Proc. Natl. Acad. Sci. USA.* 82:7149–7153.

Mikala, G., A. Bahinski, A. Yatani, S. Q. Tang, and A. Schwartz. 1993. Differential contribution by conserved glutamate residues to an ion-selectivity site in the L-type Ca^{2+} channel pore. *FEBS Lett.* 335: 265–269.

Mikami, A., K. Imoto, T. Tanabe, T. Niidome, Y. Mori, H. Takeshima, S. Narumiya, and S. Numa. 1989. Primary structure and functional expression of the cardiac dihydropyridine-sensitive calcium channel. *Nature.* 340:230–233.

Mironov, S. L. 1992. Conformational model for ion permeation in membrane channels—a comparison with multiion models and applications to calcium-channel permeability. *Biophys. J.* 63:485–496.

Momany, F. A., R. F. McGuire, A. W. Burgess, and H. A. Scheraga. 1975. Energy parameters in polypeptides. VII. Geometric parameters, partial atomic charges, nonbonded interactions, hydrogen bond interactions, and intrinsic torsional potentials of the naturally occurring amino acids. *J. Phys. Chem.* 79:2361–2381.

Nemethy, G., M. S. Pottle, and H. A. Scheraga. 1983. Energy parameters in polypeptides. 9. Updating of geometrical parameters, nonbonded interactions, and hydrogen bond interactions for the naturally occurring amino acids. *J. Phys. Chem.* 87:1883–1887.

Regulla, S., T. Schneider, W. Nastainczyk, H. E. Meyer, and F. Hofmann. 1991. Identification of the site of interaction of the dihydropyridine channel blockers nitrendipine and azidopine with the calcium-channel α_1-subunit. *EMBO J.* 10:45–49.

Strubing, C., S. Hering, and H. Glossmann. 1993. Evidence for an external location of the dihydropyridine agonist receptor site on smooth muscle and skeletal muscle calcium channels. *Br. J. Pharmacol.* 108:884–891.

Tang, S. Q., A. Yatani, A. Bahinski, Y. Mori, and A. Schwartz. 1993. Molecular localization of regions in the L-type calcium channel critical for dihydropyridine action. *Neuron.* 11:1013–1021.

Tetreault, S., and V. S. Ananthanarayanan. 1993. Interaction of calcium channel antagonists with calcium: structural studies on verapamil and its Ca^{2+} complex. *J. Med. Chem.* 36:1017–1023.

Tsien, R. W., P. T. Ellinor, and W. A. Horne. 1991. Molecular diversity of voltage-dependent Ca^{2+} channels. *Trends Pharmacol. Sci.* 12:349–354.

Tsien, R. W., P. Hess, E. W. McCleskey, and R. L. Rosenberg. 1987. Calcium channels: mechanisms of selectivity, permeation, and block. *Annu. Rev. Biophys. Biophys. Chem.* 16:265–290.

Vasquez, M., G. Nemethy, and H. A. Scheraga. 1983. Computed conformational states of the 20 naturally occurring amino acids and of the prototype residue α-aminobutyric acid. *Macromolecules.* 16:1043–1049.

Voitenco, S., S. Purnyn, I. Omelchenco, G. Dyadyusha, B. S. Zhorov, N. B. Brovtsyna, and V. I. Skok. 1991. Effect of sparteine on nicotinic acetylcholine receptors in the neurons of rat superior cervical ganglion. *Mol. Pharmacol.* 10:180–185.

Yang, J., P. T. Ellinor, W. A. Sather, J. F. Zhang, and R. W. Tsien. 1993. Molecular determinants of Ca^{2+} selectivity and ion permeation in L-type Ca^{2+} channels. *Nature.* 366:158–161.

Zhorov, B. S. 1981. Vector method for calculating derivatives of energy of atom-atom interactions of complex molecules according to generalized coordinates. *J. Struct. Chem.* 22:4–8.

Zhorov, B. S. 1993. Comparison of lowest-energy conformations of dimethylcurine and methoxyverapamil: evidence of ternary association of calcium channel, Ca^{2+}, and calcium entry blockers. *J. Membr. Biol.* 135:119–127.

Zhorov, B. S., and V. S. Ananthanarayanan. 1993. Conformational analysis of free and Ca^{2+}-bound forms of verapamil and methoxyverapamil. *J. Biomol. Struct. Dyn.* 11:529–540.

Zhorov, B. S., and V. S. Ananthanarayanan. 1994. Similarity of Ca^{2+}-bound conformations of morphine and Met-enkephalin: a computational study. *FEBS Lett.* 354:131–134.

Zhorov, B. S., and V. S. Ananthanarayanan. 1995. Computer modeling of dihydropyridines binding in the pore of a synthetic Ca^{2+} channel. *Biophys. J.* 68:A7.

Zhorov, B. S., and V. A. Govyrin. 1984. Predisposition of optimum conformations of certain adrenergic compounds to the formation of polydentate complexes with metal ions. *Dokl. Biochem.* 273:378–381.

Zhorov, B. S., and V. A. Govyrin. 1985. Chelate conformations of calcium antagonists. *In* Physico-chemical Properties of Biopolymers in Solution and Cells. A. P. Sarvazyan, editor. Institute of Biophysics of the USSR Academy of Sciences/Pushchino, Moscow Region. 160–162.